

# An Unmanned System-Guided Crowd Evacuation Method in Complex and Large-Scale Evacuation Environments

Tianrui Wu<sup>ID</sup>, Jun Yu<sup>ID</sup>, Qingchao Jiang<sup>ID</sup>, Senior Member, IEEE, and Qinjin Fan<sup>ID</sup>

**Abstract**—With the continuous expansion of the city scale and urbanization, urban road networks are becoming increasingly complex. Moreover, severe and extreme weather events, earthquakes, and other natural disasters occur frequently. Therefore, how to effectively and quickly evacuate urban crowd in dynamic environments is an urgent issue. To carry out the above objective, an unmanned system-guided crowd evacuation method is proposed in the current study. In the proposed method, the robot can perceive the environment in a timely and accurate manner to generate the evacuation map via advanced information technologies such as the Internet of Things or urban brain. Subsequently, an improved elliptic tangent graph approach based on global and local information (ETG-GLI) is utilized to plan a feasible and short evacuation path in large-scale scenarios. Finally, a novel crowd evacuation model based on the social force model is proposed to simulate the actual crowd evacuation process in complex and large-scale environments. To test the performance of the proposed path planning method, 25 different scenarios are proposed to simulate complex urban crowd evacuation environments. The experimental results show that the proposed algorithm outperforms other competitors in terms of path planning ability and computational time. Three actual evacuation cases with 324 pedestrians are modeled to further test the performance of the proposed algorithm. The simulation results demonstrate that the unmanned system-guided crowd evacuation method can find a shorter evacuation path for reducing the evacuation time in three complex and large-scale environments when compared with three other methods. Therefore, the proposed algorithm is a highly effective and promising approach to provide useful decision support and guidance for actual urban planning and urban emergency management.

Manuscript received 1 February 2024; accepted 22 February 2024. Date of publication 7 March 2024; date of current version 31 January 2025. This article was recommended for publication by Associate Editor H.-J. Kim and Editor D. Song upon evaluation of the reviewers' comments. This work was supported in part by the Humanities and Social Sciences on Planning Foundation of the Ministry of Education in China (Research on Cross-Domain Collaborative Maritime Unmanned Search and Rescue Methods and Strategies) under Grant 23YJAZH029, in part by Shanghai Pujiang Program under Grant 22PJD030, in part by the National Nature Science Foundation of China under Grant 61603244, and in part by the National Natural Science Foundation of China-Shandong Joint Fund under Grant U2006228. (*Corresponding author: Qinjin Fan*)

Tianrui Wu and Qinjin Fan are with the Logistics Research Center, Shanghai Maritime University, Shanghai 201306, China (e-mail: trwu11@126.com; forever123fan@163.com).

Jun Yu is with the Institute of Science and Technology, Niigata University, Niigata 950-2181, Japan (e-mail: yujun@ie.niigata-u.ac.jp).

Qingchao Jiang is with the Key Laboratory of Smart Manufacturing in Energy Chemical Process, Ministry of Education, East China University of Science and Technology, Shanghai 200237, China (e-mail: qchjiang@ecust.edu.cn).

This article has supplementary downloadable material available at <https://doi.org/10.1109/TASE.2024.3371102>, provided by the authors.

Digital Object Identifier 10.1109/TASE.2024.3371102

**Note to Practitioners**—In modern cities, the population density is high and the road network is complex. To evacuate the crowd in a timely and safe manner, planning feasible and short paths in large-scale and complex environments is a critical and challenging task. Therefore, the present study aims to provide a novel method to plan high-quality evacuation routes to guide the pedestrian flow. The performance of the proposed approach is validated in 25 test scenarios and 3 real-world instances. Experimental results demonstrate that the proposed algorithm performs well in terms of path length and computation time. Moreover, the proposed crowd evacuation model can simulate the actual process of crowd evacuation.

**Index Terms**—Unmanned system, crowd evacuation, path planning, ellipse tangent, large-scale environment.

## I. INTRODUCTION

**I**N RECENT years, urban areas have witnessed a surge in incidents involving crowded stampede incidents and natural disasters. For example, the New Year's Eve stampede on the bund in Shanghai resulted in 36 fatalities in 2014. Additionally, in 2021, Zhengzhou in Henan province was abruptly struck by a severe rainstorm, leading to a substantial loss of lives and properties. Another noteworthy occurrence is the crowded trampling incident that transpired in Itaewon, South Korea in 2022. Clearly, with the persistent growth of urban populations and the escalating complexity of urban road networks, the tasks of crowd evacuation and rescue have assumed paramount importance for cities in the face of emergency or unforeseen circumstances.

While numerous methodologies have been proposed in previous studies to reduce the evacuation time and enhance the evacuation safety, static evacuation planning methods face limitations when applied to large-scale, uncertain, and dynamic evacuation environments characterized by incomplete information and evolving disaster area [1], [2]. Moreover, the significance of optimizing evacuation decisions in response to the dynamic changes in the disaster area has been underscored in [3] and [4]. In other words, real-time environmental perception stands as a crucial factor ensuring the ultimate efficacy of crowd evacuation algorithms. Note that robots, equipped with advanced information technologies such as the Internet of Things (IoT) and 5G, can swiftly and comprehensively perceive environmental information. Therefore, robotic-centered unmanned systems are poised to play a crucial role in future crowd evacuation scenarios. Despite the

importance of the unmanned system-guided crowd evacuation method, it is observed that existing studies predominantly focus on simplistic and small-scale evacuation scenarios.

To address the aforementioned challenges, the present study introduces an unmanned system-guided crowd evacuation method. In this proposed approach, following the completion of environmental perception, an effective and efficient elliptic tangent graph method based on global and local information (ETG-GLI) is employed to assist robots in devising a feasible and short evacuation path within complex and large-scale evacuation environments. Subsequently, a novel social force model is incorporated to simulate real-life crowd evacuation processes and human-robot interaction (HRI). The experimental results indicate that the ETG-GLI rapidly identifies high-quality and feasible paths in complex environments. Additionally, the study incorporates three real evacuation scenarios, and simulation outcomes affirm that the proposed algorithm effectively replicates the process of actual crowd evacuation guided by a robot. Notably, it demonstrates the capability to identify optimal evacuation path in a shorter time when compared to other competitors. Therefore, the proposed algorithm provides a robust foundation for the digital twinning of large-scale urban population evacuation, assuming an important role in urban planning and disaster emergency management.

The main contributions of the current study can be summarized as follows:

(1) An efficient path planning method is proposed that utilizes both global information (i.e., the guided route from the start-point to the terminal point) and local information (i.e., the deviation degree between the sub-path and the guided route). The experimental results demonstrate that the effectiveness of the proposed path planning algorithm, showcasing its capability to successfully identify a feasible and high-quality evacuation path in complex and high-density urban areas.

(2) The current study introduces a novel crowd evacuation model that integrates following dynamics and obstacle avoidance, aiming to accurately mimic real human dispersal. Through the calculation of dynamic paths and the consideration of individual behavior, the model ensures efficient navigation during evacuations. Compared with a traditional method, the proposed evacuation model can realistically simulate human reactions to obstacles and provide a more authentic representation of the evacuation process. Therefore, it establishes a reliable foundation for the digital twinning of large-scale urban population evacuations.

(3) For artificially generated scenarios, the numerical and comparative results affirm the superior performance of the proposed path algorithm over its competitors, demonstrating advantages in both path length and run speed. Moreover, the proposed algorithm exhibits superior performance compared to three competitive algorithms when tested on three real evacuation scenarios. Therefore, the efficacy of the proposed algorithm positions it as a promising method for applications in urban planning or disaster emergency management, particularly in large-scale and high-density urban areas.

The remaining study is structured as follows. The basic methods involving social force model with obstacle avoidance

and elliptic tangent graph method are introduced in Section II. Related work is introduced in Section III. Study motivation, the proposed algorithm, and modified social force model are presented in detail in Section IV. The experimental comparisons and case studies are presented in Section V. Conclusions are given in Section VI.

## II. PRELIMINARY KNOWLEDGE

### A. Path Planning Problem

The path planning scenario in urban areas is introduced in this Subsection. When a natural disaster, such as a flood or an earthquake, occurs, urban residents need to be gathered and evacuated. Subsequently, the robots plan optimal and feasible paths to guide the crowd evacuation based on collected evacuation environmental information. Note that the three-dimensional scenario is projected into a two-dimensional one in the current study [5]. Moreover, the polygon buildings are represented as elliptical models, which helps reduce the redundancy of path planning and save computational resources. With the above considerations, the robot path planning problem can be defined as follows:

(1) For each robot, the start-point is denoted as  $S$ , and the destination is represented by  $T$ .

(2) The array of obstacles dispersed throughout the environment is symbolized by the set  $B = \{B_1, B_2, \dots, B_i, \dots, B_N\}$ , where  $N$  is the number of obstacles. An individual obstacle is marked as  $B_i$  with spatial coordinates  $(x_j, y_j)$ .

(3) A mathematical representation of the obstacle is given as follows [6]:

$$\frac{[(x - x_j) \cos \varphi + (y - y_j) \sin \varphi]^2}{(a + l_{safe})} + \frac{[(y - y_j) \cos \varphi - (x - x_j) \sin \varphi]^2}{(b + l_{safe})} = 1, \quad (1)$$

where  $a$  and  $b$  denote the major and minor axes of the ellipse, respectively;  $\varphi$  is the inclination angle of the major axis;  $l_{safe}$  defines the minimal safe distance between the robot and the obstacle, illustrating the elliptical expansion of the barrier.

Eq. (1) defines the forbidden zone for safe traversal of the robot. Subsequently, a permissible robot trajectory selected by the algorithm can be represented as the set  $\{P_0, P_1, P_2, \dots, P_n, P_{n+1}\}$ , where  $P_0$  and  $P_{n+1}$  denote the start point  $S$  and terminal point  $T$ , respectively. To obtain a collision-free path, each candidate waypoint  $P_i(x_i, y_i)$  should meet the following equation:

$$\frac{[(x_i - x_j) \cos \varphi + (y_i - y_j) \sin \varphi]^2}{(a + l_{safe})} + \frac{[(y_i - y_j) \cos \varphi - (x_i - x_j) \sin \varphi]^2}{(b + l_{safe})} \geq 1, \quad (2)$$

Besides the above constraints, other constraints can be given as follows:

(1) Endurance constraint [6]. Given the robot's energy limit, the total path length should meet the following equation:

$$D \leq D_{\max}, D = \sum_{i=1}^{m-1} d_i, \quad (3)$$

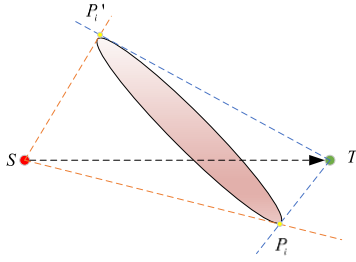


Fig. 1. The principle of elliptic tangent graph method.

where  $d_i$  as the inter-waypoint distance and  $D_{\max}$  as its maximum range.

(2) Communication constraint [7]. For a robot interfacing with devices, its route should ensure stable communication and limit interference.

(3) Movement stability constraint [8]. To ensure optimal operation and safety, a robot should satisfy the movement stability constraint. Therefore, it is assumed that the speed of the robot is constant.

### B. Elliptic Tangent Graph Method

The elliptical tangent graph method [6] introduces a refined graph-based approach that eliminates the need for extensive graph constructions. From  $S$  to  $T$ , four tangents directed towards ellipse obstacle  $B_i$  intersect, which produce two potential waypoints. As illustrated in Fig. 1, these intersections yield two candidate sub-paths, denoted as  $S \rightarrow P_i \rightarrow T$  and  $S \rightarrow P_i' \rightarrow T$ . Finally, a short path length is selected from two candidate sub-paths. Furthermore, the safety of these delineated paths can be validated by Eq. (2). Based on the above steps, the elliptical tangent graph method can generate a collision-free path from  $S$  to the  $T$  [9], [10].

### C. Social Force Model With Obstacle Avoidance

The social force model (SFM) [11] proposed by Helbing and Molnár is a famous crowd evacuation method to simulate dynamic behavior of actual crowds. The pedestrian velocity  $\vec{v}_\alpha$  based on resultant force can be calculated as follows:

$$m_\alpha \frac{d\vec{v}_\alpha(t)}{dt} = \vec{f}_\alpha^0 + \sum_{\beta(\neq\alpha)} \vec{f}_{\alpha\beta} + \sum_W \vec{f}_{\alpha w}, \quad (4)$$

where  $m_\alpha$  and  $v_\alpha$  denote the mass and velocity of the evacuee  $\alpha$ , respectively; the motion dynamics are influenced by three primary forces: the desired force  $\vec{f}_\alpha^0$ , the interaction force  $\vec{f}_{\alpha\beta}$ , and the interaction force  $\vec{f}_{\alpha w}$  between evacuee and wall. As illustrated in Fig. 2, the SFM views pedestrians as particles that are influenced by "social forces" [12].

Concretely, the desired force  $\vec{f}_\alpha^0$  is calculated as:

$$\vec{f}_\alpha^0 = m_\alpha \frac{v_\alpha^0(t) \vec{e}_\alpha^0(t) - \vec{v}_\alpha(t)}{\tau_\alpha}, \quad (5)$$

where  $v_\alpha^0$  denotes the preferred speed of the evacuee  $\alpha$ ;  $\vec{e}_\alpha^0$  is the desired unit direction vector of the evacuee  $\alpha$ ;  $\vec{v}_\alpha$  represents the current velocity of the evacuee  $\alpha$ ;  $\tau_\alpha$  denotes

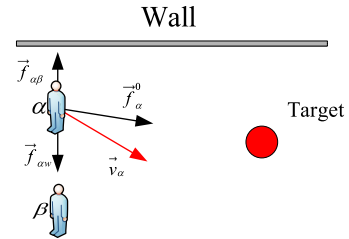


Fig. 2. The social force model.

the reaction time of the evacuee  $\alpha$ . The interaction force  $\vec{f}_{\alpha\beta}$  between the evacuee  $\alpha$  and the evacuee  $\beta$  is expressed by:

$$\vec{f}_{\alpha\beta} = A_\alpha e^{\frac{r_{\alpha\beta}-d_{\alpha\beta}}{B_\alpha}} \vec{n}_{\alpha\beta} + kg(r_{\alpha\beta}-d_{\alpha\beta}) \vec{n}_{\alpha\beta} + \kappa g(r_{\alpha\beta}-d_{\alpha\beta}) \Delta v_{\beta\alpha}^t \vec{t}_{\alpha\beta}, \\ g(x) = \begin{cases} x, & x > 0 \\ 0, & x \leq 0, \end{cases} \quad (6)$$

where  $A_\alpha e^{\frac{r_{\alpha\beta}-d_{\alpha\beta}}{B_\alpha}} \vec{n}_{\alpha\beta}$ ,  $kg(r_{\alpha\beta}-d_{\alpha\beta}) \vec{n}_{\alpha\beta}$ , and  $\kappa g(r_{\alpha\beta}-d_{\alpha\beta}) \Delta v_{\beta\alpha}^t \vec{t}_{\alpha\beta}$  are the repulsive interaction force, the body contact force, and the sliding friction force, respectively;  $A_\alpha$  and  $B_\alpha$  are constants at the strength and range of the repulsive force;  $r_{\alpha\beta}$  is the sum of two evacuees' radii;  $d_{\alpha\beta}$  is the Euclidean distance between the evacuee  $\alpha$  and the evacuee  $\beta$ ;  $\vec{n}_{\alpha\beta}$  denotes a unit vector pointing from the evacuee  $\alpha$  to the evacuee  $\beta$ ;  $\Delta v_{\beta\alpha}^t \vec{t}_{\alpha\beta}$  refers to the speed gap in tangential orientation between the evacuee  $\alpha$  and the evacuee  $\beta$ ;  $k$  and  $\kappa$  are two constants; Similarly, the interaction force  $\vec{f}_{\alpha w}$  between the evacuee  $\alpha$  and wall can be computed as follows:

$$\vec{f}_{\alpha w} = A_\alpha e^{\frac{r_{\alpha w}-d_{\alpha w}}{B_\alpha}} \vec{n}_{\alpha w} + kg(r_\alpha-d_{\alpha w}) \vec{n}_{\alpha w} + \kappa g(r_\alpha-d_{\alpha w}) \Delta v_{w\alpha}^t \vec{t}_{\alpha w}, \quad (7)$$

where  $r_\alpha$  is radius of the evacuee  $\alpha$ ;  $d_{\alpha w}$  represents the distance from the evacuee  $\alpha$  to the wall;  $\vec{n}_{\alpha w}$  denotes a unit vector oriented from the evacuee  $\alpha$  towards the wall;  $\Delta v_{w\alpha}^t \vec{t}_{\alpha w}$  refers to the speed gap in tangential orientation between the evacuee  $\alpha$  and the wall.

In the traditional SFM, the obstacle avoidance behavior of pedestrians is not considered. Therefore, the improved version of the SFM [13] that incorporates obstacle avoidance provides a more accurate depiction of pedestrian behavior, which can be defined as:

$$m_\alpha \frac{d\vec{v}_\alpha(t)}{dt} = \vec{f}_\alpha^0 + \sum_{\beta(\neq\alpha)} \vec{f}_{\alpha\beta} + \sum_W \vec{f}_{\alpha w} + \sum_O \vec{f}_{\alpha o}, \quad (8)$$

where  $\vec{f}_{\alpha o}$  represents the repulsion from the obstacle and is expressed as follows:

$$\vec{f}_{\alpha o} = \frac{2m_\alpha (\vec{B}_{\alpha o} - \vec{D}_{\alpha o} - \vec{v}_{\alpha o} \Delta t)}{(\Delta t)^2}, \quad (9)$$

where vector  $\vec{B}_{\alpha o}$  denotes buffer vector from the obstacle to evacuee  $\alpha$ ;  $\vec{v}_{\alpha o}$  denotes an orthogonal speed to the obstacle;  $\vec{D}_{\alpha o}$  indicates the direction from the obstacle to evacuee  $\alpha$ ;  $\Delta t$  represents the movement interval.

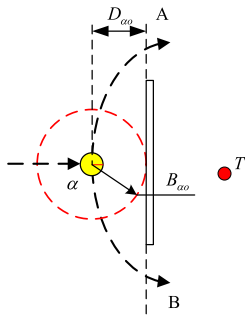


Fig. 3. Impact of obstacle on the evacuee  $\alpha$ .

Based on [13] and [14], different obstacle avoidance behavior of pedestrians (see Fig. 4) is given as follows:

(1) If no obstacles are detected, then the objective of the evacuee  $\alpha$  is to reach the  $T$ .

(2) If an obstacle is encountered and influenced by the resultant force, the trajectory of the evacuee  $\alpha$  redirects towards either side A or B.

(3) After circumventing the obstacle, the evacuee  $\alpha$  reorients towards the  $T$ .

As illustrated in Fig. 3, the evacuee  $\alpha$  is influenced by both the resultant force and the local information within the vision field, thus the evacuee  $\alpha$  will choose the lower channel B to bypass the obstacle.

### III. RELATED WORK

Due to high building density, urbanization, and diverse requirements at different time periods and locations, metropolitan regions are susceptible to hazards such as traffic congestion, earthquakes, floods, and so on [15]. Therefore, selecting an appropriate evacuation scheme to minimize the loss of life and property is vital. To carry out the above objective, Fragkos et al. [3] introduced a novel evacuation-planning mechanism, which is named as the ESCAPE. In the proposed algorithm, the reinforcement learning and game theory are utilized to aid and distribute decision-making autonomously during evacuations. The ESCAPE is evaluated through simulations to showcase its effectiveness and advantages in various scenarios. Zhou et al. [16] designed a multimodal cooperative guidance (MMCG) system to enhance evacuation efficiency and safety in a subway station. Within this system, they proposed a bi-level MMCG optimization model and extended social force model for evacuation dynamics. The results demonstrate that the proposed algorithm can enhance evacuation efficiency and exit utilization. Ma et al. [17] proposed a joint data and service evacuation scheme for cloud data centers to improve survivability in the face of disasters. Moreover, the integer linear program (ILP) models and heuristic rules are involved in resource sharing. The numerical results demonstrate that the scheme can offer a practical approach for data center operators under resource and time constraints. Wang et al. [18] modified the SFM by the adaptive parameters to disperse evacuees through narrow exits. The simulation experiments show that the bottleneck length less than 2m negatively affects evacuation efficiency in an indoor scenario. When the bottleneck length is longer, the pedestrian flow tends

to exhibit a more uniform distribution. To alleviate bottleneck congestion in metro stations during peak hours, Peng et al. [19] proposed a system dynamic-based framework to optimize the aisle length. Moreover, they defined the key bottleneck region and employed the system dynamic model for simulation. The experiment indicates that a minimum aisle length of 6m is needed for the efficient operation of the passenger flow. In [20], safety evacuation signs (SESs) are integrated into a crowd simulation method for emergency situations. This method blends real-world SESs functions into a virtual environment to determine efficient, conflict-free evacuation routes. The effectiveness of the proposed method confirmed through extensive simulations demonstrates its capability of handling complex path planning problems interactively for multiple groups. To minimize evacuation time, Yang et al. [21] developed a multi-objective optimization model that considers traffic capacity at nodes and employs the back propagation (BP) neural network. The model, validated by simulation, significantly improves the evacuation efficiency by 21.85%. Li et al. [22] proposed a risk assessment approach using convolutional neural networks (CNN) to rapidly anticipate risks during evacuation. By training the model with real-case data from a large stadium, the study proves that the deep learning method can provide valuable decision support for evacuation decision-making. To improve disaster management, He et al. [23] proposed a cellular automata-based dynamic route optimization (CADRO) algorithm to find an evacuation path when a flood occurs. Experiments conducted in a suburb of Yangzhou City show that the proposed CADRO can significantly shorten the length of evacuation routes when compared with the traditional A\* algorithm. In Ref. [24], the shelter location problem is formulated as a network flow model, and then a minimum-cost-maximum-flow solution approach is proposed. This approach aims to optimize pedestrian evacuation in urban areas during natural disasters. The results demonstrate the effectiveness of the proposed algorithm in improving human behavior during evacuations. Additionally, the emergency disaster evacuation is often determined by considering various factors, such as the disaster magnitude, data collection for evacuation planning, and transportation management. To this end, an emergent intelligence (EI) technique-based transport management proposed by Chavhan and Venkataram [15] is utilized to assist evacuees in moving from a disaster zone to a safe zone. The proposed method has been tested in a case study. The experimental results demonstrate that their algorithm can reduce the delay of the disaster information propagation, save the evacuation time, and facilitate a uniform distribution of victims among evacuation exit points. In Ref. [25], questionnaires and geographic information system (GIS) methods are modified to alleviate the challenges of assessing seismic urban evacuation behavior. Based on the assessment results, metropolitan seismic safe zone layout and urban planning can be developed to enhance the urban disaster guard capability. In order to balance spatiotemporal attributes of urban area evacuation, Jiang et al. [26] built a large-scale multimodal transport macro-optimization evacuation method to address the spatiotemporal coordination issue of multiple transportation modes during evacuation. Experimental results from on a

realistic incident demonstrate that the multimodal transport evacuation can distinctly improve efficiency compared with a single transport evacuation method. Chen et al. [27] proposed an improved model to address the time-consuming estimation and assessment of evacuation bottleneck in urban areas. The simulation results show that the proposed model can numerically evaluate the evacuation vulnerability and help in emergency management and prevention of crowd emergencies. To minimize the negative impacts of the pluvial flood, Borowska-Stefanska et al. [28] developed a four-step traffic model that considers the entire national traffic system. The analysis results show that the shortest route may be the preferred selection under normal conditions, while it may not be the optimal route during flooding events. Therefore, using different information is important for making evacuation plans.

Besides the above studies, robots have been used to guide the crowd evacuation in recent years. For example, to enhance the positive impact of robots on pedestrian flow, Zhang et al. [29] investigated the influence of robot settings on pedestrian and crowd dynamics. Moreover, they designed the test involving 28 human participants and two different types of robots. The qualitative results show that pedestrians tend to interact with wheelchair robot more conservatively and follow certain “social rules” compared to the humanoid robot. To reduce evacuation costs, Lu et al. [30] introduced a stochastic optimal intervention method for implementing robot-assisted crowd evacuation. In the proposed algorithm, the stochastic evolution rules and the Hamilton-Jacobi-Bellman (HJB) equation are utilized to obtain optimal intervention strategies. The experimental results show the proposed method can alleviate the “chaos” phenomena and improve the evacuation efficiency. In Ref. [31], a stochastic differential equation model is developed to optimize the positioning of robots and select appropriate human-robot interactions for efficient and safe evacuation of human crowds. Simulations are provided to demonstrate the effectiveness of their proposed method and confirm using multiple robots can greatly facilitate the process of human crowd evacuation. The method of mobile robot-guided evacuation, proposed by Boukas et al. [32], aims to deal with the risks associated with crowd gathering. The results demonstrate that the proposed method not only evaluates human behavior in emergency situations, but also utilizes a simultaneous localization and mapping algorithm to find collision-free routes for guiding evacuees. For the purpose of employing robots to influence the crowds through HRI, Wan et al. [33] developed a deep reinforcement learning method to model the process of robot assisting pedestrian regulation in the L-shape cloister. The obtained results show that the robot optimal motion decisions can improve the pedestrian flow. In Ref. [34], an adaptive dynamic programming approach is used for robot-assisted pedestrian regulation. This improves learning efficiency and reduces the need for offline training in deep neural networks. Comprehensive simulation studies are conducted using a robotic simulator to validate the proposed approach and assess its performance. Robotic simulator tests show that the method effectively regulates pedestrian flows to prevent potential disasters. To dynamically optimize human behavior during

emergencies in a complex indoor environment, Tang et al. [35] quantified mental panic and incorporated it into the SFM, and then a robot is used to guide evacuees to safety. Through simulations conducted in commercial complexes, robot-assisted evacuation system proves effective in alleviating crowd congestion. In Ref. [36], a robot-guided crowd evacuation model is used to improve the passenger evacuation at the railway hub station during emergency situations. The experimental results demonstrate that the proposed method can aid in finding the optimal evacuation route while also mitigating potential risks.

Based on the above introductions, finding optimal and feasible evacuation paths in the crowd evacuation is an important yet challenging issue. To achieve the above objective, a large number of path planning methods have been proposed in previous studies. For example, Liu et al. [6] proposed two autonomous path planning algorithm (SETG-TG, DETG-TG) based on a tangent intersection and target guidance strategy. The experimental results demonstrate that the SETG-TG algorithm can efficiently generate collision-free paths in static environments outperforming other algorithms. Meanwhile, the DETG-TG algorithm excels in real-time adaptation to unforeseen obstacles without needing advance environment data. In Ref. [37], the trajectory and wireless resource allocation of drones are optimized to ensure the timely data collection from IoT devices in areas with limited or low-quality wireless coverage. Through extensive simulation and analysis, the results indicate that the proposed algorithm outperforms other two greedy algorithms in terms of distance and deadline. To achieve the rapid and reliable transmission of emergency information, Huang et al. [38] proposed an UAV path planning framework involving waypoint and motion. The system optimizes UAV positioning for reliable data transmission and speeds up waypoint traversal for maximum data collection. The experimental results prove that the proposed algorithm can offer a scientific management for the post-disaster emergency response. In Ref. [39], two offline collision-avoidance multi-drone path-planning algorithms (DETACH, STEER) are proposed to address the collision problems among multiple UAVs. The DETACH and STEER aim to maximize waypoint coverage per flight path by the nearest-neighbor search algorithm. Compared with traditional methods, two proposed algorithms can operate more UAVs in a wider area with the same available resources. To obtain energy-efficient and collision-avoidance routes in complex environments, Kyaw et al. [40] proposed an modified batch informed trees\* algorithm (BIT\*) which integrates a knowledgeable planner with energy objectives for each of the robot’s reconfigurable actions. The results show that the proposed algorithm can generate optimal paths with low energy consumption and demonstrates the superior performance in real-world scenarios. Moreover, swarm intelligence methods have been widely used in the field of path planning. To achieve an effective planner for a UAV in a complex environment, Chai et al. [41] proposed the multi-strategy fusion differential evolution algorithm (MSFDE), in which the multi-population strategy, the self-adaptive strategy, and the ensemble of the interactive mutation strategy are used. The simulation results demonstrate that the proposed algorithm outperforms

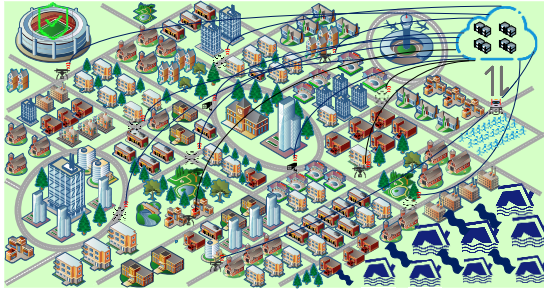


Fig. 4. The unmanned system for urban crowd evacuation.

other competitors in complex three-dimensional path planning environments.

#### IV. PROPOSED METHODS

##### A. Study Motivation

Traditional crowd evacuation methods have obvious limitations. For example, stationary signs, while cost-effective, are greatly affected by environmental changes and psychological factors [42]. Additionally, the human guidance method is capable of reducing the evacuation time due to known environments, but these leaders require extensive training and may not be well-suited for changing and complex environments, especially in large-scale scenarios. Expanding city scales and increasingly complex road networks in urban growth necessitate a reconsideration of evacuation strategies [43]. Therefore, there are two challenging tasks in the urban crowd evacuation: (1) existing methods for crowd evacuation may not be suitable for complex dynamic scenarios, such as traditional leader or landmark strategies. Therefore, robust environmental perception capability is a prerequisite for the successful application of the unmanned system-guided crowd evacuation method. Furthermore, path planning algorithms must be efficient and capable of meeting real-time requirements. Therefore, it is crucial to develop efficient and fast-solving path planning algorithms; and (2) simple and small-scale scenarios are often focused in previous studies, thus complex and large-scale evacuation scenarios should be considered in the actual evacuation of urban populations. Moreover, these scenarios can provide more effective and useful decision support for urban planning or disaster emergency management.

Unlike human leaders and signs, intelligent agents [44], [45], possess real-time and powerful environmental perception capabilities in advanced information technology and artificial intelligence environments [46], [47]. In the current study, the agent can be an intelligent robot or drone, which combines real-time information of urban buildings and road networks. Furthermore, the evacuation path and the crowd guidance method can be generated based on the heuristic information. As shown in Fig. 4, an unmanned system-based crowd evacuation method can leverage various advanced information technologies such as the IoT and 5G to comprehensively perceive dynamic/uncertain environments. Moreover, the cloud computing [48], edge computing [49], and other methods can be employed to help plan evacuation paths. Finally, allowing intelligent agents to execute evacuation tasks. Therefore,

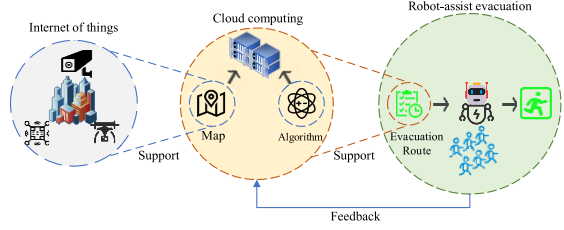


Fig. 5. Framework of unmanned system-based crowd evacuation method.

various advanced robot technologies can be integrated into the proposed method, such as navigation, control, human-robot interaction, etc. The general framework of the proposed method is illustrated in Fig. 5. It can be observed from Fig. 5 that the information collection and transmission can be achieved via IoT and 5G on the perception side. On the information processing side, path planning algorithms can utilize high-performing computing technologies like the cloud computing for computation. On the execution side, various types of intelligence agents can be used to guide urban crowd evacuation. It should be noted that the human-computer interaction technology can also be used for information interaction and sharing between humans and the unmanned system to enhance the environmental perception and decision-making capabilities. Therefore, developing an unmanned system-guided crowd evacuation method is important for actual disaster management.

##### B. Robot-Guidance Social Force Model

Different from the traditional leader/signage guidance, the robots are used to guide the crowd evacuation in the present study. Compared with leaders/signage, robots can comprehensively perceive the evacuation environments and quickly respond based on advanced information technologies such as the IoT and cloud computing. Furthermore, the SFM is utilized to simulate the evacuation process of each pedestrian following the robot or the adjacent crowd. Additionally, the visual range of each pedestrian includes both a radius and an angle, as detailed in Ref. [50]. Therefore, the adopted SFM can be formulated as follows:

$$m_\alpha \frac{d\vec{v}_\alpha(t)}{dt} = m_\alpha \frac{v_\alpha^0(t)\vec{e}_\alpha^0(t) - \vec{v}_\alpha(t)}{\tau_\alpha} + \sum_{\beta \in VF_\alpha} \vec{f}_{\alpha\beta} + \sum_{W \in VF_\alpha} \vec{f}_{\alpha w} + \sum_{O \in VF_\alpha} \vec{f}_{\alpha o} + \sum_{r \in VF_\alpha} \vec{f}_{\alpha r}, \quad (10)$$

where  $VF_\alpha$  is the visual field of the evacuee  $\alpha$ ;  $\vec{f}_{\alpha r}$  denotes the repulsive force between pedestrian  $\alpha$  and the robot, which is calculated by:

$$\vec{f}_{\alpha r} = A_\alpha e^{\frac{r_\alpha - d_{\alpha r}}{B_\alpha}} \vec{n}_{\alpha r} + kg(r_\alpha - d_{\alpha r}) \vec{n}_{\alpha r} + \kappa g(r_\alpha - d_{\alpha r}) \Delta v_{\alpha r}^t \vec{t}_{\alpha r}, \quad (11)$$

where  $d_{\alpha r}$  denotes the distance from the evacuee  $\alpha$  to the robot;  $\vec{n}_{\alpha r}$  is a directional vector initiating from the evacuee  $\alpha$  to the robot;  $\Delta v_{\alpha r}^t \vec{t}_{\alpha r}$  describes the tangential speed difference between the evacuee  $\alpha$  and the robot.

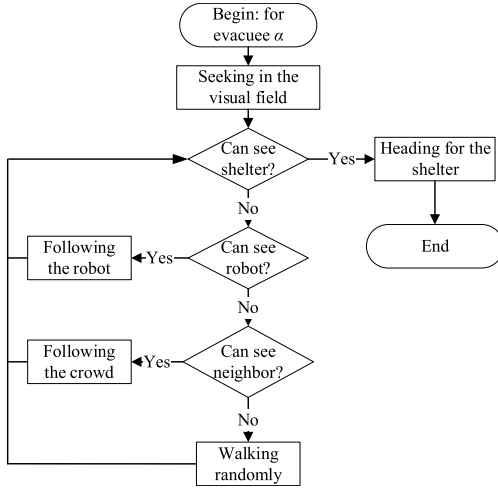


Fig. 6. Flowchart of evacuee's decision in visual field.

Urban crowd evacuation is achieved in a dynamic and complex environment, thus evacuees' desired directions can be defined as follows [50]:

$$\vec{e}_\alpha^0 = \begin{cases} \text{Norm}[p_s - p_\alpha(t)], & \text{If the evacuee } \alpha \text{ detects a shelter} \\ \text{Norm}[p_r(t) - p_\alpha(t)], & \text{If the evacuee } \alpha \text{ detects a robot} \\ \text{Norm}[\gamma \vec{e}_\alpha^i(t) + (1 - \gamma) \vec{e}_\alpha^j(t)], & \text{If the evacuee } \alpha \text{ detects a crowd} \\ \text{Rand}(\vec{n}), & \text{If the evacuee } \alpha \text{ does not detect anything,} \end{cases} \quad (12)$$

where  $p_s$ ,  $p_r(t)$ , and  $p_\alpha(t)$  indicate the location of the shelter, the position of robot, and the evacuee  $\alpha$  at  $t$  time;  $\vec{e}_\alpha^i(t)$  and  $\vec{e}_\alpha^j(t)$  are the average orientation of the neighbor crowd and the direction of the crowd's center, respectively;  $\gamma$  denotes the balanced parameter;  $\vec{n}$  is a unit vector. The flowchart of evacuee's decision in the visual field is shown in Fig. 6.

We can observe from Eq. (12), evacuees guided by robots are influenced by navigational forces. This leads to changes in movement speeds and a reorientation towards the robot's intended path. During the evacuation process, evacuees may experience one of the following scenarios [14], [51], [52]:

(1) If the evacuee  $\alpha$  can see the shelter within their visual field, a direct route toward the shelter is taken.

(2) If the evacuee  $\alpha$  can detect the presence of the robot, the follow-the-robot behavior is exhibited.

(3) If the evacuee  $\alpha$  can perceive neighboring peers, the "follow the crowd" principle is exhibited.

(4) If the evacuee  $\alpha$  lacks discernible guiding cues, the "random walking" strategy is taken.

Meanwhile, to eliminate the interference of accidental factors during the evacuation process, several assumptions are made as follows [36], [53], [54].

(1) The crowd and the robot interact through hierarchical relationship [55].

(2) The pedestrians always trust the guidance of the robot.

### Algorithm 1 ETG-GLI

---

**Input:** Starting point  $S$ , Terminal point  $T$

- 1 Construct the map constituted of elliptical obstacles
- 2 Initialize:  $P_g \leftarrow [S]$ ,  $P_a \leftarrow [T]$ ,  $O_k \leftarrow \emptyset$ ,  $D_k \leftarrow \emptyset$ ,  $B_{OD}(k) \leftarrow \emptyset$ ,  $k \leftarrow 1$
- 3 **While**  $k < K$
- 4   **While**  $P_a$  is not empty
- 5      $O_k \leftarrow P_g(\text{end})$ ,  $D_k \leftarrow P_a(\text{end})$ , and obtain guided path  $O_k D_k$
- 6     Search the obstacles passed by  $O_k D_k$ , and add the order of obstacles needed avoided into  $B_{OD}(k)$
- 7     **If**  $B_{OD}(k)$  is empty
- 8       Add  $D_k$  to  $P_g$ , and delete  $D_k$  from  $P_a$
- 9     **Else**
- 10       Generate four tangents of the obstacle from  $O_k$  and  $D_k$  respectively, and obtain two candidate waypoint  $P_i$  and  $P'_i$ . Subsequently, the global offset angle  $\theta_i$  is achieved by calculating  $O_k P_i$  and  $ST$ , and the global offset angle  $\theta'_i$  is calculated via  $O_k P_i'$  and  $ST$ .
- 11       **If**  $\theta_i < \theta'_i$
- 12         Add the waypoint  $P_i$  to  $P_s(k)$
- 13       **Else**
- 14         Add the waypoint  $P'_i$  to  $P_s(k)$
- 15     **End if**
- 16     **If**  $O_k P_s(k)$  is collision-free
- 17       Add the  $P_s(k)$  to  $P_g$
- 18     **Else**
- 19       Add the  $P_s(k)$  to  $P_a$
- 20     **End if**
- 21   **End if**
- 22   **End while**
- 23    $k = k+1$
- 24 **End while**
- 25 Utilize the cubic B-spline curve method to smooth the path

**Output:** The optimized path for robot

---

(3) The robot's commands and behavior are controlled by the unmanned system.

### C. The Elliptic Tangent Graph Based on Global and Local Information

In the unmanned system-guided crowd evacuation method, after completing the environmental perception, planning feasible and optimal evacuation routes in a complex and large-scale environment is one of the most important and challenging tasks. To this end, the elliptic tangent graph based on global and local information (ETG-GLI) algorithm is proposed to solve the robot path planning problem in complex and large-scale evacuation environments. Nomenclature definitions are listed in Table I.

The pseudocode of the proposed ETG-GLI is described in **algorithm 1**. The main steps of the ETG-GLI algorithm are described as follows:

*Step 1:* Obstacles in the environment are modeled as ellipses based on Eq. (1) (Line 1). Initialize  $O_k$ ,  $D_k$ ,  $P_g$ ,  $P_a$ ,  $k$ , and  $B_{OD}(k)$ . Set  $S$  to  $P_g(\text{end})$  and  $T$  to  $P_a(\text{end})$  (Line 2).

*Step 2:* Define  $O_k$  as  $P_g(\text{end})$  and  $D_k$  as  $P_a(\text{end})$ , and obtain guided path  $O_k D_k$  (Line 5). Then, detect the obstacles needed avoided along  $O_k D_k$  and record them into  $B_{OD}(k)$  (Line 6). If  $B_{OD}(k)$  is empty, then the  $D_k$  is inserted into the  $P_g$  and delete it from  $P_a$  (Line 8). Otherwise, generate four tangents to avoid the obstacle from  $O_k$  and  $D_k$ , respectively. Namely, two alternative waypoints can be obtained. To find a short path, the global offset angle  $\theta_j$  is achieved by calculating  $O_k P_i$

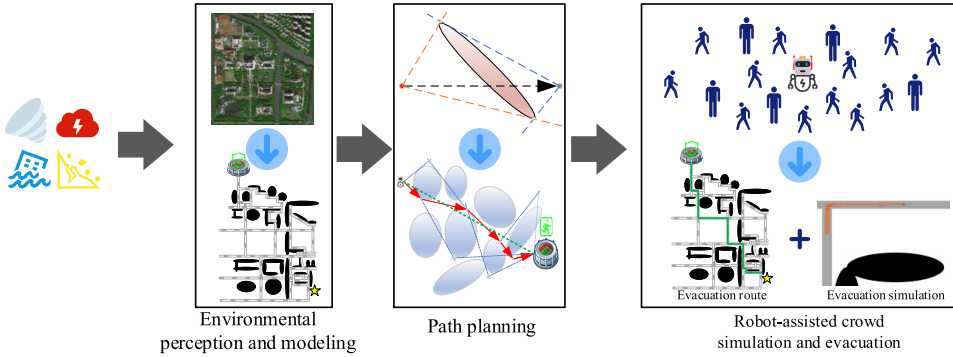


Fig. 7. Overall implementation of the proposed algorithm.

TABLE I  
NOMENCLATURE DEFINITIONS OF ETG-GLI

Nomenclature	Description
$S, T, ST$	a starting point, a terminal point, the global guidance
$O_k, D_k$	the origin-point in the $k$ th iteration, the destination-point in the $k$ th iteration
$O_k D_k$	the navigation path in the $k$ th iteration
$P_i, P'_i$	two alternative waypoints in the $k$ th iteration
$O_k P_i, O'_k P'_i$	the origin sub-paths in the $k$ th iteration
$D_k P_i, D'_k P'_i$	the destination sub-paths in the $k$ th iteration
$P_s(k)$	a set of waypoints selected to be the planned path in the $k$ th iteration
$P_g$	a set of global generated waypoints
$P_a$	a set of alternative sub-path waypoints
$B_{OD}(k)$	a set of the avoided obstacles in the $k$ th iteration

and  $ST$ , and the global offset angle  $\theta'_i$  is calculated via  $O_k P'_i$  and  $ST$ . Lines 11-15 are to select a candidate waypoint via the global offset angles. If  $\theta_i < \theta'_i$ , the waypoint  $P_i$  is added in  $P_s(k)$ ; otherwise, the waypoint  $P'_i$  is added in  $P_s(k)$ . Lines 16-20 aim to assess the feasibility of the  $O_k P_s(k)$ . If  $O_k P_s(k)$  is collision-free, then add the waypoint  $P_s(k)$  to the set  $P_g$ . Otherwise, add the waypoint  $P_s(k)$  to the  $P_a$ . Repeat lines 4-23 until  $k > K$ . After completing the above steps, the cubic B-spline curve [56], [57] is employed to smooth the obtained path.

*Step 3:* Output a collision-free and optimal path to the robot for implementing urban crowd evacuation.

#### D. Overall Implementation of the Proposed Algorithm

Based on the above descriptions, the overall implementation of the unmanned system-guided crowd evacuation method is illustrated in Fig. 7. It can be observed from Fig. 7 that the proposed method mainly consists of three parts: (1) environmental perception and modeling; (2) path planning; (3) robot-assisted crowd simulation and evacuation. To effectively complete the disaster response, the evacuation map is firstly modeled via the environmental perception. Then, the proposed ETG-GLI is used to plan a feasible and short path in complex and large-scale evacuation environments. Based on the obtained candidate waypoints, the intersection selection and GIS technology [58] are employed to form a feasible evacuation route. Finally, a robot-assisted crowd evacuation method is employed to simulate real-life robot-guided crowd evacuation process.

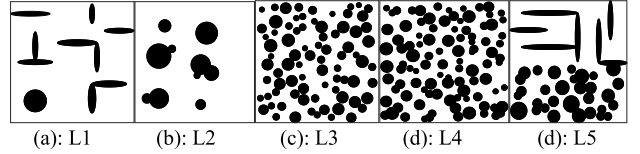


Fig. 8. Five different types of obstacle layouts.

## V. EXPERIMENTAL RESULTS AND ANALYSES

### A. Scenario and Parameter Settings

To demonstrate the effectiveness of the proposed ETG-GLI, four competitive path planning algorithms including A\* [59], RRT [60], PMR [61] and SETG-TG [6] are used in the experiments. Moreover, five different typical obstacle layout scenarios (marked as L1, L2, L3, L4 and L5 [62]), which are illustrated in Fig. 8, are selected to test the performance of all compared algorithms. These five types of obstacle layouts can change in terms of density and overlap. L1 has non-overlapping bar and circular obstacles; L2 includes intersecting circles; L3 has non-intersecting circles; intersecting circles are involved in L4; and L5 integrates intersecting circles with corridors.

Based on the above five different types of obstacle layouts, 25 scenarios are used in experiments. The more details are given in Table S-1 in the supplementary file. The size of I1-I15 is 100 m \* 100 m, and starting and terminal points in I11-I15 are different. Moreover, the size of the I16-I25 is 200 m \* 200 m. For the ETG-GLI, the maximum iteration is set to 1000. For all compared algorithms, run times are set to be 30 on each instance, and the parameter settings in the compared algorithms are in accordance with their original studies.

### B. Experimental Comparison

In this Subsection, the proposed ETG-GLI is compared with four path planning methods on 25 instances. The values of the average and standard deviation obtained by the proposed ETG-GLI and four competitive path planning approaches are reported in Table II. The best results are shown in bold. In addition, the Holm-Bonferroni test [63] method is employed to analyze the obtained results. '+' , '-' , and '=' denote the performance of the comparison algorithm is superior, inferior, or comparable to the ETG-GLI, respectively.

TABLE II  
THE PATH LENGTH OF ALL COMPARED ALGORITHMS ON 25 INSTANCES

Instance	A*	PMR	RRT	SETG-TG	ETG-GLI
I1	1.9510e+02 (1.2524e+00)	+ (3.5190e+00)	1.6150e+02 (1.5820e+01)	2.1086e+02 (1.4052e+00)	<b>1.5049e+02</b> <b>(1.4052e+00)</b>
I2	1.9475e+02 (1.5174e+00)	+ (1.2054e+00)	1.4875e+02 (1.0535e+01)	1.8197e+02 (1.6205e+00)	1.5591e+02 (1.6465e+00)
I3	1.9465e+02 (1.1367e+00)	+ (4.8667e-01)	1.4832e+02 (1.3359e+01)	1.8561e+02 (3.5169e+00)	1.5489e+02 (1.4422e+00)
I4	1.9530e+02 (1.1743e+00)	+ (1.1679e+00)	1.4433e+02 (3.9083e+00)	1.6489e+02 (1.4253e+00)	1.4777e+02 (1.4827e+02)
I5	1.9715e+02 (7.4516e-01)	+ (1.4961e+00)	1.6742e+02 (6.4519e+00)	1.8009e+02 (2.2912e+00)	1.5268e+02 (1.4530e+00)
I6	1.9460e+02 (1.5355e+00)	+ (1.9542e-01)	1.6305e+02 (1.1342e+01)	1.7130e+02 (1.2440e+00)	1.4966e+02 (1.1140e+00)
I7	1.9500e+02 (1.5560e+00)	+ (6.2726e-01)	1.7156e+02 (1.6099e+01)	1.9514e+02 (1.3229e+00)	1.4891e+02 (1.4519e+02)
I8	1.9710e+02 (1.0712e+00)	+ (1.0495e+00)	1.5789e+02 (1.0310e+01)	1.6818e+02 (5.3119e+00)	1.6987e+02 (1.4662e+02)
I9	1.9513e+02 (1.2677e+00)	+ (2.6663e-01)	1.7188e+02 (3.2042e+01)	2.1416e+02 (3.6627e+00)	1.6603e+02 (1.4593e+00)
I10	1.6653e+02 (1.5223e+00)	+ (5.0811e-01)	1.5101e+02 (2.1142e+01)	2.1395e+02 (1.3276e+00)	1.5960e+02 (1.5420e+02)
I11	1.8254e+02 (7.5371e-01)	+ (1.2154e+00)	1.7527e+02 (1.7627e+00)	2.1083e+02 (9.2466e-01)	2.2130e+02 (1.6721e+02)
I12	1.8338e+02 (5.9506e-01)	+ (1.5997e+00)	1.5330e+02 (1.1434e+01)	2.5326e+02 (4.1128e+01)	1.7048e+02 (1.6339e+02)
I13	1.8500e+02 (7.9472e-01)	+ (3.3219e-01)	1.3465e+02 (8.2558e-01)	2.1110e+02 (4.9341e-01)	1.1767e+02 (1.2042e+02)
I14	2.3355e+02 (1.2763e+00)	+ (1.5961e+00)	1.8005e+02 (1.3201e+01)	2.2857e+02 (4.8880e-01)	1.7012e+02 (1.6385e+02)
I15	2.1105e+02 (9.4451e-01)	+ (1.5925e-01)	2.5495e+02 (1.4850e+00)	1.9652e+02 (4.9629e-01)	1.4508e+02 (1.4205e+02)
I16	3.9620e+02 (1.0052e+00)	+ (3.5416e+00)	2.9863e+02 (1.7713e+01)	3.6009e+02 (5.8888e-01)	3.2562e+02 (3.0956e+02)
I17	3.9825e+02 (1.0195e+00)	+ (7.9451e-01)	3.4846e+02 (3.4509e+00)	3.9996e+02 (1.4258e+00)	3.3903e+02 (2.9533e+02)
I18	3.9640e+02 (2.5005e+00)	+ (9.2283e-01)	3.5521e+02 (1.7861e+01)	4.0277e+02 (1.2661e+00)	3.5895e+02 (2.8988e+02)
I19	5.0585e+02 (1.0400e+00)	+ (9.1974e-01)	3.4355e+02 (4.2120e+01)	4.0947e+02 (1.4785e+00)	3.3288e+02 (2.9019e+02)
I20	3.9785e+02 (1.0417e+00)	+ (2.6757e+00)	3.9590e+02 (6.0886e+00)	3.8772e+02 (1.8202e+00)	3.5905e+02 (1.4285e+00)
I21	3.9570e+02 (1.1286e+00)	+ (7.6340e-01)	2.8903e+02 (1.4661e+01)	3.4069e+02 (1.3925e+00)	3.2436e+02 (2.8791e+02)
I22	5.2005e+02 (1.0501e+00)	+ (7.8969e-01)	3.3364e+02 (3.2243e+01)	3.8239e+02 (1.7847e+00)	3.0505e+02 (2.9131e+02)
I23	4.1400e+02 (8.5840e-01)	+ (8.1330e-01)	3.5196e+02 (2.4935e+01)	3.9469e+02 (1.3815e+00)	3.1674e+02 (2.9445e+02)
I24	3.9855e+02 (8.8704e-01)	+ (8.8326e-01)	3.2446e+02 (1.2101e+01)	3.8146e+02 (3.6279e+01)	3.1370e+02 (2.9318e+02)
I25	4.4250e+02 (1.0000e+00)	+ (9.0471e-01)	3.7876e+02 (2.7468e+01)	4.1062e+02 (1.5801e+00)	3.1504e+02 (2.9059e+02)
+/-/-		25/0/0	25/0/0	25/0/0	23/2/0    -/-/-

It can be observed from Table II that the proposed ETG-GLI outperforms the A\* algorithm, PRM, and RRT on all scenarios. The main reason may be that the proposed ETG-GLI employs the global and local information to find a feasible and optimal path. For the A\* algorithm, the information of the full map can be extracted to find a collision-free route, but it explores the search space based on the estimated cost to the goal state and considers only those paths that are likely to result in a suboptimal solution. For the PRM and RRT, although they are commonly used to plan paths in robotics and autonomous systems, random sampling may limit their search capability, especially in complex environments with narrow passages or tight spaces. Also, Table II indicates that the performance of the ETG-GLI is significantly better than that of the SETG-TG on 25 scenarios. Moreover, their performances are the similar on two scenarios, i.e., L1 and L4. Therefore, the overall performance of the ETG-GLI is significantly better than that of the SETG-TG.

Beside the path length, the response time is a critical metric in the case of emergency evacuations. Therefore, a short computational time is crucial for path planning algorithms. The computational time of all compared algorithms are presented

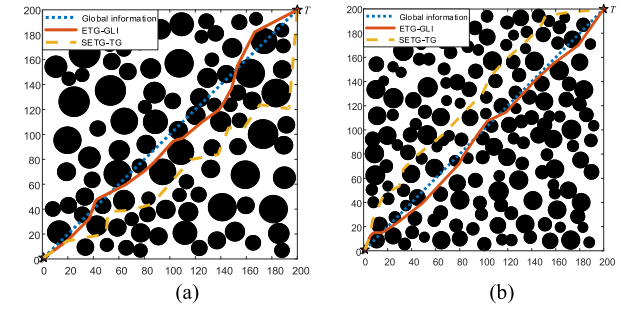


Fig. 9. Path generated by ETG-GLI and SETG-TG in I17 and I23.

in Table S-2 in the attachment file. It can be seen from Table S-2 that the proposed algorithm has a significantly advantage in terms of computational time when compared with other competitors. Although the proposed algorithm uses more computational time than the RRT and SETG-TG in a few scenarios, their difference is acceptable.

To visually compare the performance of the ETG-GLI and the SETG-TG, two complex scenarios I17 and I23 are selected in this experiment. The paths of these two algorithms are illustrated in Fig. 9. Clearly, it can be observed from Fig. 9 that

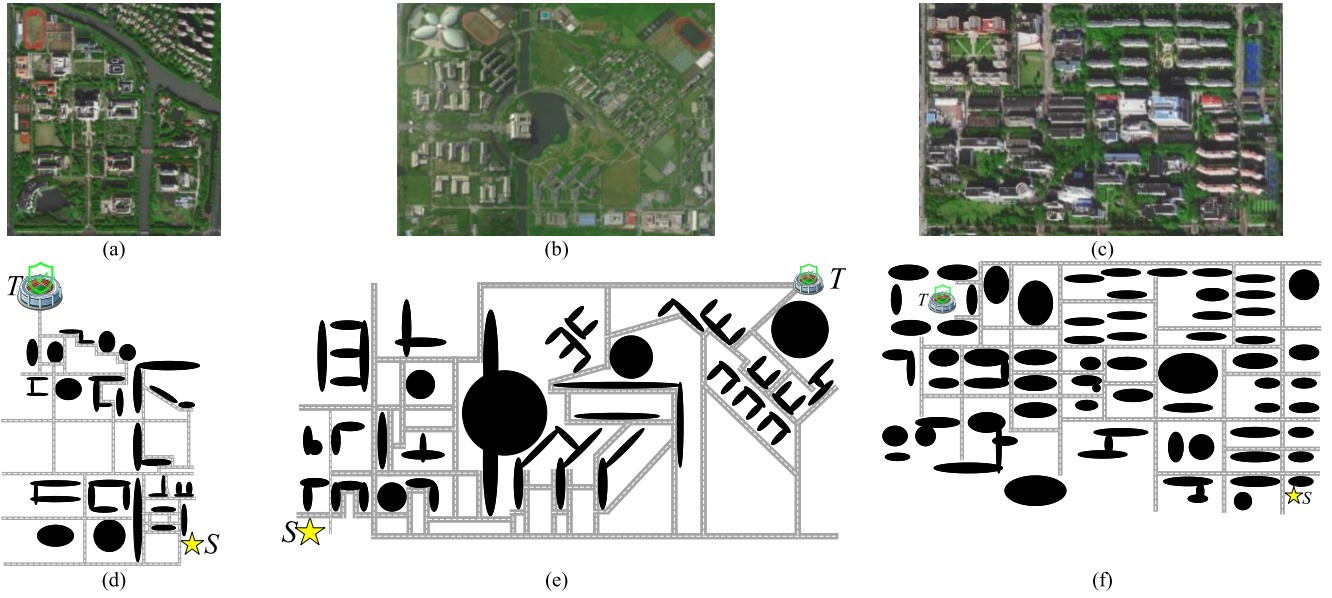


Fig. 10. Three scenarios for urban crowd evacuation.

the ETG-GLI is more promising path planning method to find a feasible and high-quality evacuation path when compared with the SETG-TG.

In summary, the ETG-GLI shows great potential in planning safe and efficient routes in various complex evacuation environments and is capable of meeting the computational time requirements for urban crowd evacuation scenarios. Therefore, the proposed algorithm is a useful and reliable method to solve different types of evacuation environments.

### C. Case Study

Experimental comparisons in Subsection V-B are mainly used to verify the path planning capability of the proposed algorithm. However, like the path planning algorithm, it is also crucial to demonstrate the proposed crowd evacuation model, as it is utilized to simulate the actual evacuation process in the unmanned system-guided crowd evacuation system. Therefore, both the path planning algorithm and the crowd evacuation model are tested in this Subsection.

**1) Three Evacuation Scenarios:** In the current study, three large-scale and complex urban evacuation environments are used. The settings including the number of obstacle (i.e., Num\_obstacle) of three cases are shown in Table III. The three actual evacuation scenarios are illustrated in Figs. 10 (a), (b), and (c), and three simplified ones are shown in Figs. 10 (d), (e) and (f). It can be observed from Fig. 10 that the task of the robot in the unmanned system-assisted crowd evacuation is to evacuate the crowd from a high-risk area (i.e., S) to the shelter (i.e., T). Note that the obstacles such as buildings, revers, and lakes are represented as ellipses based on Eq. (1). Additionally, the objective in Fig. 10 is to use the robot for guiding crowd from a high-risk area to a shelter in the shortest possible time. The first step of the proposed algorithm is to complete environmental perception, and then the proposed path planning algorithm is utilized to find a safe and short evacuation path. Moreover, the proposed crowd evacuation

TABLE III  
SETTINGS OF THREE EVACUATION ENVIRONMENTS

Case	Starting point	Shelter location	Num. obstacle	Aera(m <sup>2</sup> )
1	(680,50)	(80,960)	39	700000
2	(36,40)	(1440, 760)	69	1280000
3	(700,40)	(130,360)	73	337500

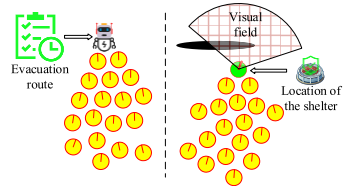


Fig. 11. Two different guidance methods in the unmanned system and human avoidance evacuation strategies.

model can be utilized to simulate the evacuation process of urban populations.

**2) Parameter Settings in Crowd Evacuation Model:** The parameter settings of the crowd evacuation model are shown in Table IV. Moreover, parameter settings for each pedestrian are the same in [13] and [50]: the body radius is 0.6m, the mass is 80kg, the reaction time is 0.5s, and the desired walking speed is 1.5m/s. Notably, all 324 evacuees are uniformly distributed in the initial state.

**3) Experimental Comparisons:** As mentioned above, the human guidance and signage are the two main methods for crowd evacuation in previous studies. However, signage cannot be used to evacuate the crowd in large-scale crowd evacuation scenarios. Therefore, a human guidance strategy (see Fig. 11) [64], the spherical vector-based particle swarm optimization (SPSO) [65] and the SETG-TG [6] are used to compare with the performance of the proposed method in the experiments. For the human guidance strategy, the leader tends to choose the closer path to avoid obstacles based on the information perceived within the visual field. It can be observed from Fig. 11 that the crowd is followed by the human leader in the traditional method, while the robot is employed to guide

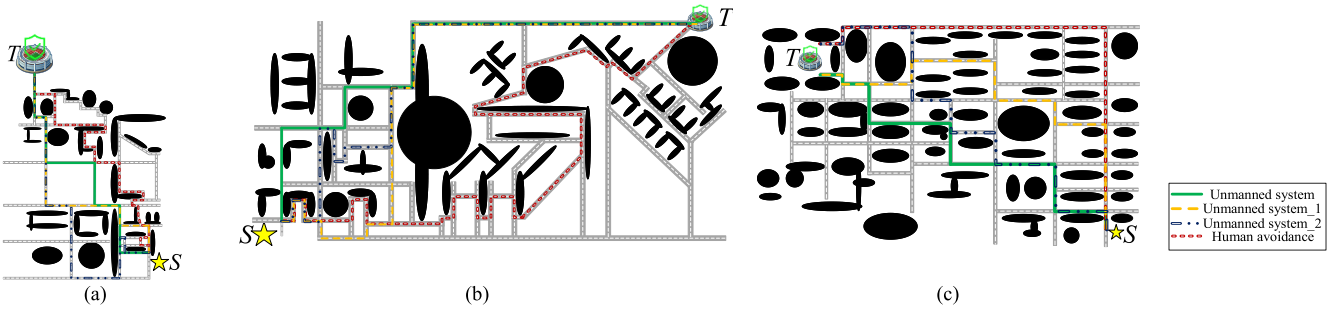


Fig. 12. Paths for four evacuation strategies and three algorithms in C1, C2 and C3.

TABLE IV

PARAMETER SETTINGS OF THE SOCIAL FORCE MODEL

Parameter	Meaning	Value
$VF_r$	Radius of visual field	6m
$VF_a$	Angle of visual field	120°
$A_a$	Repulsive interaction	2000N
$B_a$	Range of repulsive interaction	0.08m
$\kappa$	Coefficient of sliding friction	$3.0 \times 10^4 \text{ kg}/(\text{m} \cdot \text{s})$
$k$	Coefficient of body compression	$2.0 \times 10^4 \text{ kg}/\text{s}^2$
$B_{oo}$	Range of obstacle interaction	1.5m

TABLE V  
PATH LENGTH UNDER THREE METHODS

Case	Path length under human avoidance(m)	Path length under unmanned system_1(m)	Path length under unmanned system_2(m)	Path length under unmanned system(m)
1	1736	1387	1762	1387
2	3045	2217	2353	2079
3	990	948	990	872

the crowd evacuation in the proposed algorithm. Additionally, the SPSO (named as unamend system\_1) and the SETG-TG (named as unamend system\_2) also used to demonstrate the performance of the proposed algorithm in this experiment. For the SPSO, the maximum number of function evaluations and the population size are set to 300,000 and 500, respectively. Moreover, three compared algorithms are independently run ten times in each scenario.

The mean values of path length achieved by three compared algorithms are shown in Table V. It can be observed from Table V that, compared with the human guidance strategy, the proposed algorithm reduces the path lengths by 349m, 966m, and 118m in these three scenarios, respectively. Namely, the proposed algorithm reduces the path lengths by 20.1%, 31.7%, and 11.9% in these three evacuation scenarios, respectively, compared with the traditional human guidance method. Specifically, the proposed method achieves more competitive results than the human guidance method in case 2 (shown in Fig. 10 (e)), which is the most complex in among all scenarios. The main reason may be that, compared with the human guidance strategy, the proposed algorithm not only has a high-performance path planning algorithm, but also can perceive the evacuation environment, which provides effective help for solving the problem of difficult to obtain complete information about environmental changes.

As shown in Table V, the proposed method outperforms the unamend system\_1 in cases 2 (shown in Fig. 10 (e)) and 3 (shown in Fig. 10 (f)), with the same result in scenario 1 (shown in Fig. 10 (d)). For the case 1, the evacuation

TABLE VI  
AVERAGE RUN TIME OF TWO ALGORITHMS ON THREE CASES

Case	SPSO(s)	SETG-TG(s)	ETG-GLI(s)
1	78.155732	0.005829	<b>0.004021</b>
2	74.159104	0.006998	<b>0.005068</b>
3	86.600269	0.009629	<b>0.009356</b>

environment is relatively simple, thus the proposed algorithm and the unamend system\_1 can achieve the same optimal result. However, the proposed algorithm performs better than the unamend system\_1 in two remaining scenarios. This means that the proposed algorithm has a superior path planning capability when solving complex evacuation scenarios. Meanwhile, the proposed algorithm generates shorter evacuation paths in three cases when compared with the unamend system\_2. Therefore, like the results shown in Table II, the proposed algorithm can find a shorter path in complex scenarios. Additionally, Table VI also shows that the run time of the proposed algorithm is slightly shorter than that of the SETG-TG. Clearly, the proposed algorithm is capable of planning a high-quality evacuation path in the shortest time possible, which is crucial for crowd evacuation in emergency scenarios. Through comprehensive comparisons, the proposed algorithm demonstrates its effectiveness and promise as a method to evacuate urban crowds in large-scale and complex scenarios.

To visually compare the performance of all compared algorithms, the actual evacuation paths obtained by three compared algorithms are illustrated in Fig. 12. The proposed algorithm outperforms the unamend system\_2 in the actual urban networks (shown in Fig. 12). It can be observed from Fig. 12(a) that, although the proposed algorithm and the unamend system\_1 find different evacuation paths, their path lengths are the same. However, the human guidance strategy can only perceive local information, which leads to the phenomenon of “detour”. For two complex evacuation scenarios, Figs. 12 (b) and (c) show that the proposed algorithm can plan a shorter evacuation path for the robot to evacuate the crowd. Therefore, it can be concluded that the strong environmental perception and the high-performance path planning algorithm are two essential capabilities for realizing crowd evacuation in large-scale and complex scenarios.

Based on the above experimental comparisons and analyses, we can conclude that the proposed path planning method is a competitive and reliable approach to find a short evacuation path in complex environments. This not only improves evacuation efficiency, but also enhances the safety in emergency situations.

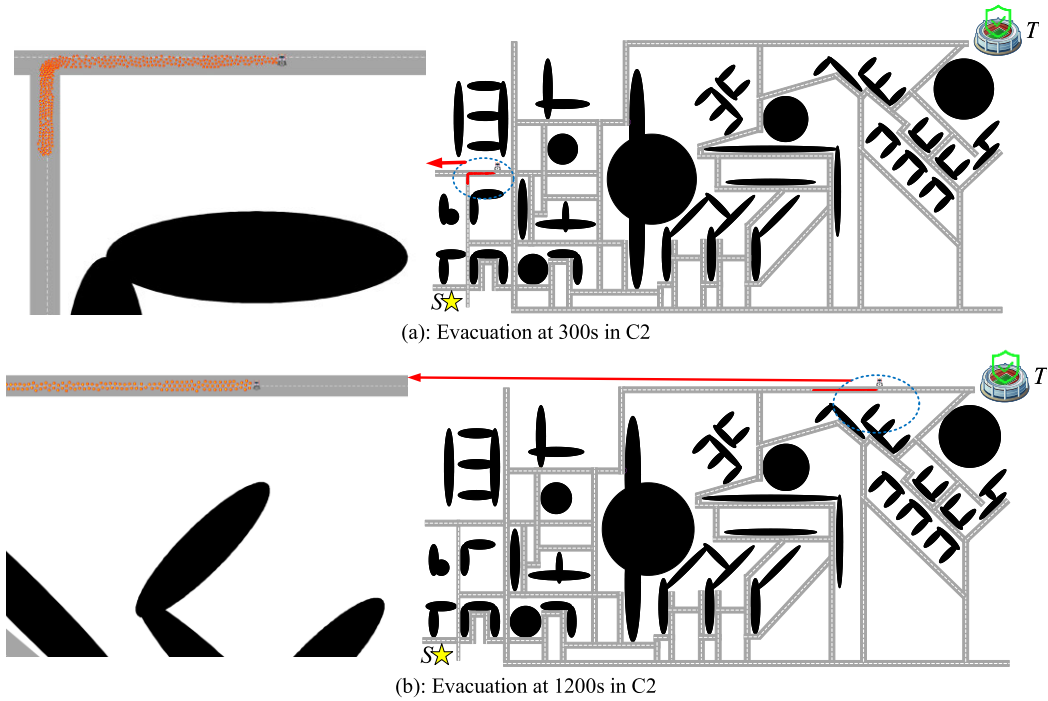


Fig. 13. The snapshots of the unmanned system-guide crowd evacuation in C2.

**4) Effectiveness of Proposed Crowd Evacuation Model:** To demonstrate the effectiveness of the proposed crowd evacuation model, the three typical crowd evacuation scenarios (i.e., the evacuation time is 300s and 1200s) are shown in Fig. 13. It can be observed from Fig. 13(a) that the crowd is able to evacuate along with the robot at the corner and effectively simulate the process of real-life crowd evacuation. Notably, bottlenecks and congestion are likely to occur at the corner due to the abrupt change in the movement direction. The crowd exhibits “herding behavior” [66], as guided by the robot. The individuals reciprocally mimic and gradually aggregate based on the states of their neighbors and the robot, which forms a self-organized and cohesive pedestrian evacuation flow. Fig. 13(b) also shows that the proposed crowd evacuation model can accurately simulate the process of the crowd evacuation on the straight pathway. Based on the above analyses, it can be concluded that the proposed crowd evacuation model can accurately simulate the actual processes of the crowd evacuation. This can provide a reliable foundation for the digital twinning of large-scale urban population evacuation.

## VI. CONCLUSION

To achieve the efficient and rapid evacuation of urban crowd in complex and large-scale evacuation environment, the unmanned system-guided crowd evacuation method is proposed in the present study. In the proposed algorithm, an enhanced elliptic tangent graph approach based on global and local information (ETG-GLI) is used to plan a short and feasible path for evacuation robots. Moreover, a novel crowd evacuation model based on the social force model is proposed to simulate the actual crowd evacuation process in large-scale and intricate environments. The effectiveness of the proposed path planning method is assessed through 25 distinct

complex urban crowd evacuation environments. The results indicate that the proposed algorithm outperforms other competitors in terms of path planning capability and computation time. Furthermore, three real-life evacuation cases involving 324 pedestrians are used to test the performance of the proposed algorithm. The simulations reveal that the unmanned system-guided crowd evacuation method reduced evacuation path length by 20.1%, 31.7% and 11.9% in three large-scale and complex environments compared to the traditional leader guidance. Moreover, the proposed algorithm outperforms the selected swarm intelligence algorithm in two complex scenarios and achieves the same result in one scenario. Also, the proposed algorithm has a great advantage in terms of computational time. Compared with the SETG-TG algorithm, the proposed algorithm also performs better in three actual evacuation scenarios. Because the proposed algorithm can be used for digital twin or simulation experiments, it can provide useful guidance for the real-world urban planning and the disaster management. Meanwhile, the proposed social force model is able to effectively simulate the impact of leader and demonstrate human local obstacle avoidance based on information in the visual field. Therefore, the unmanned system-guided method is a highly effective and promising tool for simulating actual crowd evacuation processes and reducing the evacuation time in large-scale and complex urban evacuation scenarios.

The current study focused on a single robot-assisted crowd evacuation, thus we plan to develop multi-robot path planning methods to evacuate crowds in future study. Moreover, the evacuees and urban environments considered in the current study are relatively simple, and we will consider other factors such as evacuees’ psychological factors, physiological factors, and urban roads in the future. Finally, we will use the

proposed algorithm in the digital twinning of large-scale urban population evacuation or other real-world scenarios such as urban planning and urban emergence management.

## REFERENCES

- [1] K. Shahabi and J. P. Wilson, "Scalable evacuation routing in a dynamic environment," *Comput., Environ. Urban Syst.*, vol. 67, pp. 29–40, Jan. 2018.
- [2] Q. Lu, B. George, and S. Shekhar, "Capacity constrained routing algorithms for evacuation planning: A summary of results," in *Proc. 9th Int. Symp. Spat. Temp. Dbs. (SSTD)*, 2005, pp. 291–307.
- [3] G. Frakos, P. Apostolopoulos, and E. Tsipropoulou, "ESCAPE: Evacuation strategy through clustering and autonomous operation in public safety systems," *Future Internet*, vol. 11, no. 1, p. 20, Jan. 2019.
- [4] A. Bahamid, A. M. Ibrahim, and A. A. Shafie, "Crowd evacuation with human-level intelligence via neuro-symbolic approach," *Adv. Eng. Informat.*, vol. 60, Apr. 2024, Art. no. 102356.
- [5] Z. Yao, W. Zhang, Y. Shi, M. Li, Z. Liang, and Q. Huang, "ReinforcedRimJump: Tangent-based shortest-path planning for two-dimensional maps," *IEEE Trans. Ind. Informat.*, vol. 16, no. 2, pp. 949–958, Feb. 2020.
- [6] H. Liu, X. Li, M. Fan, G. Wu, W. Pedrycz, and P. N. Suganthan, "An autonomous path planning method for unmanned aerial vehicle based on a tangent intersection and target guidance strategy," *IEEE Trans. Intell. Transp. Syst.*, vol. 23, no. 4, pp. 3061–3073, Apr. 2022.
- [7] U. Kim et al., "A novel intrinsic force sensing method for robot manipulators during human–robot interaction," *IEEE Trans. Robot.*, vol. 37, no. 6, pp. 2218–2225, Dec. 2021.
- [8] Z. Miao, W. Huang, Q. Jiang, and Q. Fan, "A novel multi-modal multi-objective optimization algorithm for multi-robot task allocation," *Trans. Inst. Meas. Control*, early access, Jun. 2023, Art. no. 0142312231183588, doi: [10.1177/0142312231183588](https://doi.org/10.1177/0142312231183588).
- [9] H. Chen, K. Chang, and C. S. Agate, "UAV path planning with tangent-plus-Lyapunov vector field guidance and obstacle avoidance," *IEEE Trans. Aerosp. Electron. Syst.*, vol. 49, no. 2, pp. 840–856, Apr. 2013.
- [10] Y. Liu, Q. Wang, H. Hu, and Y. He, "A novel real-time moving target tracking and path planning system for a quadrotor UAV in unknown unstructured outdoor scenes," *IEEE Trans. Syst. Man, Cybern. Syst.*, vol. 49, no. 11, pp. 2362–2372, Nov. 2019.
- [11] D. Helbing and P. Molnár, "Social force model for pedestrian dynamics," *Phys. Rev. E, Stat. Phys. Plasmas Fluids Relat. Interdiscip. Top.*, vol. 51, no. 5, pp. 4282–4286, May 1995.
- [12] K. Deng, X. Hu, M. Li, and T. Chen, "An extended social force model considering the psychological impact of the hazard source and its behavioural manifestation," *Phys. A, Stat. Mech. Appl.*, vol. 627, Oct. 2023, Art. no. 129127.
- [13] T. Wu, Q. Liu, W. Wang, and Q. Fan, "Layout optimization of indoor obstacle using a multimodal multi-objective evolutionary algorithm," in *Proc. 12th Int. Conf. Swarm Intell. (ICSI)*, 2022, pp. 534–544.
- [14] W.-L. Wang, H.-C. Li, J.-Y. Rong, Q.-Q. Fan, X. Han, and B.-H. Cong, "A modified heuristics-based model for simulating realistic pedestrian movement behavior," *Chin. Phys. B*, vol. 31, no. 9, Sep. 2022, Art. no. 094501.
- [15] S. Chavhan and P. Venkataram, "Transport management for evacuation of victims," *IEEE Trans. Emerg. Topics Comput. Intell.*, vol. 5, no. 3, pp. 426–441, Jun. 2021.
- [16] M. Zhou, H. Dong, P. A. Ioannou, and F.-Y. Wang, "Crowd evacuation with multi-modal cooperative guidance in subway stations: Computational experiments and optimization," *IEEE Trans. Computat. Social Syst.*, vol. 10, no. 5, pp. 2536–2545, Aug. 2023.
- [17] L. Ma, W. Su, B. Wu, B. Yang, and X. Jiang, "Joint emergency data and service evacuation in cloud data centers against early warning disasters," *IEEE Trans. Netw. Service Manage.*, vol. 19, no. 2, pp. 1306–1320, Jun. 2022.
- [18] J. Wang et al., "A modified universal pedestrian motion model: Revisiting pedestrian simulation with bottlenecks," *Building Simul.*, vol. 15, no. 4, pp. 631–644, Apr. 2022.
- [19] J. Peng, Z. Wei, Y. Yang, W. Wang, S. Qiu, and S. Wang, "What size of aisle is necessary? A system dynamics model for mitigating bottleneck congestion in entrance Halls of metro stations," *IEEE Trans. Intell. Transp. Syst.*, vol. 23, no. 12, pp. 22923–22936, Dec. 2022.
- [20] L. Lyu, C. Pang, and J. Wang, "Virtual-real syncretic crowd simulation method guided by building safety evacuation sign," *IEEE Sensors J.*, vol. 23, no. 16, pp. 18486–18499, Jul. 2023.
- [21] X. Yang, Y. Yang, D. Qu, X. Chen, and Y. Li, "Multi-objective optimization of evacuation route for heterogeneous passengers in the metro station considering node efficiency," *IEEE Trans. Intell. Transp. Syst.*, vol. 24, no. 11, pp. 12448–12461, Nov. 2023.
- [22] J. Li, Y. Hu, and J. Li, "Rapid risk assessment of emergency evacuation based on deep learning," *IEEE Trans. Computat. Social Syst.*, vol. 9, no. 3, pp. 940–947, Jun. 2022.
- [23] M. He et al., "An efficient dynamic route optimization for urban flooding evacuation based on cellular automata," *Comput., Environ. Urban Syst.*, vol. 87, May 2021, Art. no. 101622.
- [24] J. G. Jin, Y. Shen, H. Hu, Y. Fan, and M. Yu, "Optimizing underground shelter location and mass pedestrian evacuation in urban community areas: A case study of Shanghai," *Transp. Res. A, Policy Pract.*, vol. 149, pp. 124–138, Jul. 2021.
- [25] C. Chen and L. Cheng, "Evaluation of seismic evacuation behavior in complex urban environments based on GIS: A case study of Xi'an, China," *Int. J. Disaster Risk Reduction*, vol. 43, Feb. 2020, Art. no. 101366.
- [26] J. Jiang, W. Tu, H. Kong, W. Zeng, R. Zhang, and M. Konecny, "Large-scale urban multiple-modal transport evacuation model for mass gathering events considering pedestrian and public transit system," *IEEE Trans. Intell. Transp. Syst.*, vol. 23, no. 12, pp. 23059–23069, Dec. 2022.
- [27] J. Chen et al., "An enhanced model for evacuation vulnerability assessment in urban areas," *Comput., Environ. Urban Syst.*, vol. 84, Nov. 2020, Art. no. 101540.
- [28] M. Borowska-Stefánska et al., "Emergency management of self-evacuation from flood hazard areas in Poland," *Transp. Res. D, Transp. Environ.*, vol. 107, Jun. 2022, Art. no. 103307.
- [29] B. Zhang, J. Amirian, H. Eberle, J. Pettré, C. Holloway, and T. Carlson, "From HRI to CRI: Crowd robot interaction—Understanding the effect of robots on crowd motion," *Int. J. Social Robot.*, vol. 14, no. 3, pp. 631–643, Apr. 2022.
- [30] D. Lu, G. Zhang, and X. Jia, "Stochastic optimal intervention for robot-assisted crowd evacuation," *IEEE Trans. Intell. Transp. Syst.*, early access, Oct. 27, 2023, doi: [10.1109/TITS.2023.3325424](https://doi.org/10.1109/TITS.2023.3325424).
- [31] Z. Liu, B. Wu, and H. Lin, "Coordinated robot-assisted human crowd evacuation," in *Proc. IEEE Conf. Decis. Control (CDC)*, Dec. 2018, pp. 4481–4486.
- [32] E. Boukas, I. Kostavelis, A. Gasteratos, and G. C. Sirakoulis, "Robot guided crowd evacuation," *IEEE Trans. Autom. Sci. Eng.*, vol. 12, no. 2, pp. 739–751, Apr. 2015.
- [33] Z. Wan, C. Jiang, M. Fahad, Z. Ni, Y. Guo, and H. He, "Robot-assisted pedestrian regulation based on deep reinforcement learning," *IEEE Trans. Cybern.*, vol. 50, no. 4, pp. 1669–1682, Apr. 2020.
- [34] C. Jiang, Z. Ni, Y. Guo, and H. He, "Pedestrian flow optimization to reduce the risk of crowd disasters through human–robot interaction," *IEEE Trans. Emerg. Topics Comput. Intell.*, vol. 4, no. 3, pp. 298–311, Jun. 2020.
- [35] B. Tang, C. Jiang, H. He, and Y. Guo, "Human mobility modeling for robot-assisted evacuation in complex indoor environments," *IEEE Trans. Human-Mach. Syst.*, vol. 46, no. 5, pp. 694–707, Oct. 2016.
- [36] M. Zhou, H. Dong, S. Ge, X. Wang, and F.-Y. Wang, "Robot-guided crowd evacuation in a railway hub station in case of emergencies," *J. Intell. Robotic Syst.*, vol. 104, no. 4, p. 67, Apr. 2022.
- [37] M. Samir, S. Sharafeddine, C. M. Assi, T. M. Nguyen, and A. Ghrayeb, "UAV trajectory planning for data collection from time-constrained IoT devices," *IEEE Trans. Wireless Commun.*, vol. 19, no. 1, pp. 34–46, Jan. 2020.
- [38] Z. Huang, C. Chen, and M. Pan, "Multiobjective UAV path planning for emergency information collection and transmission," *IEEE Internet Things J.*, vol. 7, no. 8, pp. 6993–7009, Aug. 2020.
- [39] K. Shen, R. Shivan, J. Medina, Z. Dong, and R. Rojas-Cessa, "Multidepot drone path planning with collision avoidance," *IEEE Internet Things J.*, vol. 9, no. 17, pp. 16297–16307, Sep. 2022.
- [40] P. T. Kyaw et al., "Energy-efficient path planning of reconfigurable robots in complex environments," *IEEE Trans. Robot.*, vol. 38, no. 4, pp. 2481–2494, Aug. 2022.
- [41] X. Chai et al., "Multi-strategy fusion differential evolution algorithm for UAV path planning in complex environment," *Aerospace Sci. Technol.*, vol. 121, Feb. 2022, Art. no. 107287.
- [42] M. Zhou, H. Dong, X. Wang, X. Hu, and S. Ge, "Modeling and simulation of crowd evacuation with signs at subway platform: A case study of Beijing subway stations," *IEEE Trans. Intell. Transp. Syst.*, vol. 23, no. 2, pp. 1492–1504, Feb. 2022.

- [43] M. Zhou, H. Dong, P. A. Ioannou, Y. Zhao, and F.-Y. Wang, "Guided crowd evacuation: Approaches and challenges," *IEEE/CAA J. Autom. Sinica*, vol. 6, no. 5, pp. 1081–1094, Sep. 2019.
- [44] S. Gronauer and K. Diepold, "Multi-agent deep reinforcement learning: A survey," *Artif. Intell. Rev.*, vol. 55, no. 2, pp. 895–943, 2022.
- [45] J. Sharma, P.-A. Andersen, O.-C. Granmo, and M. Goodwin, "Deep Q-learning with Q-matrix transfer learning for novel fire evacuation environment," *IEEE Trans. Syst. Man. Cybern. Syst.*, vol. 51, no. 12, pp. 7363–7381, Dec. 2021.
- [46] Y. Zhu, D. Zhao, and H. He, "Optimal feedback control of pedestrian flow in heterogeneous corridors," *IEEE Trans. Autom. Sci. Eng.*, vol. 18, no. 3, pp. 1097–1108, Jul. 2021.
- [47] P. A. Apostolopoulos, G. Fragkos, E. E. Tsipropoulou, and S. Papavassiliou, "Data offloading in UAV-assisted multi-access edge computing systems under resource uncertainty," *IEEE Trans. Mobile Comput.*, vol. 22, no. 1, pp. 175–190, Jan. 2023.
- [48] C. Wu, A. N. Toosi, R. Buyya, and K. Ramamohanarao, "Hedonic pricing of cloud computing services," *IEEE Trans. Cloud Comput.*, vol. 9, no. 1, pp. 182–196, Jan. 2021.
- [49] S. Wang et al., "A cloud-guided feature extraction approach for image retrieval in mobile edge computing," *IEEE Trans. Mobile Comput.*, vol. 20, no. 2, pp. 292–305, Feb. 2021.
- [50] Y. Ma, E. W. M. Lee, and M. Shi, "Dual effects of guide-based guidance on pedestrian evacuation," *Phys. Lett. A*, vol. 381, no. 22, pp. 1837–1844, Jun. 2017.
- [51] Z.-M. Huang, W.-N. Chen, Q. Li, X.-N. Luo, H.-Q. Yuan, and J. Zhang, "Ant colony evacuation planner: An ant colony system with incremental flow assignment for multipath crowd evacuation," *IEEE Trans. Cybern.*, vol. 51, no. 11, pp. 5559–5572, Nov. 2021.
- [52] G. H. Subramanian, N. Choubey, and A. Verma, "Modelling and simulating serpentine group behaviour in crowds using modified social force model," *Phys. A, Stat. Mech. Appl.*, vol. 604, Oct. 2022, Art. no. 127674.
- [53] Y. Ji, Y. Yang, F. Shen, H. T. Shen, and X. Li, "A survey of human action analysis in HRI applications," *IEEE Trans. Circuits Syst. Video Technol.*, vol. 30, no. 7, pp. 2114–2128, Jul. 2020.
- [54] P. B. Luh, C. T. Wilkie, S.-C. Chang, K. L. Marsh, and N. Olderman, "Modeling and optimization of building emergency evacuation considering blocking effects on crowd movement," *IEEE Trans. Autom. Sci. Eng.*, vol. 9, no. 4, pp. 687–700, Oct. 2012.
- [55] S. Saunderson and G. Nejat, "Robots asking for favors: The effects of directness and familiarity on persuasive HRI," *IEEE Robot. Autom. Lett.*, vol. 6, no. 2, pp. 1793–1800, Apr. 2021.
- [56] M. Elbanhawi, M. Simic, and R. N. Jazar, "Continuous path smoothing for car-like robots using B-Spline curves," *J. Intell. Robotic Syst.*, vol. 80, no. S1, pp. 23–56, Dec. 2015.
- [57] T. Berglund, A. Brodnik, H. Jonsson, M. Staffanson, and I. Soderkvist, "Planning smooth and obstacle-avoiding B-spline paths for autonomous mining vehicles," *IEEE Trans. Autom. Sci. Eng.*, vol. 7, no. 1, pp. 167–172, Jan. 2010.
- [58] R. Tamakloe, J. Hong, J. Tak, and D. Park, "Finding evacuation routes using traffic and network structure information," *Transp. Res. D, Transp. Environ.*, vol. 95, Jun. 2021, Art. no. 102853.
- [59] P. E. Hart, N. J. Nilsson, and B. Raphael, "A formal basis for the heuristic determination of minimum cost paths," *IEEE Trans. Syst. Sci. Cybern.*, vol. SCS-4, no. 2, pp. 100–107, Jul. 1968.
- [60] D. Devaurs, T. Siméon, and J. Cortés, "Optimal path planning in complex cost spaces with sampling-based algorithms," *IEEE Trans. Autom. Sci. Eng.*, vol. 13, no. 2, pp. 415–424, Apr. 2016.
- [61] L. E. Kavraki, P. Svestka, J.-C. Latombe, and M. H. Overmars, "Probabilistic roadmaps for path planning in high-dimensional configuration spaces," *IEEE Trans. Robot. Autom.*, vol. 12, no. 4, pp. 566–580, Aug. 1996.
- [62] E. G. Tsardoulias, A. Iliakopoulou, A. Kargakos, and L. Petrou, "A review of global path planning methods for occupancy grid maps regardless of obstacle density," *J. Intell. Robotic Syst.*, vol. 84, nos. 1–4, pp. 829–858, Dec. 2016.
- [63] S. Holm, "A simple sequentially rejective multiple test procedure," *Scandin. J. Statist.*, vol. 6, no. 2, pp. 65–70, 1979.
- [64] G.-Q. He, Y. Yang, Z.-H. Chen, C.-H. Gu, and Z.-G. Pan, "A review of behavior mechanisms and crowd evacuation animation in emergency exercises," *J. Zhejiang Univ. Sci. C*, vol. 14, no. 7, pp. 477–485, Jul. 2013.
- [65] M. D. Phung and Q. P. Ha, "Safety-enhanced UAV path planning with spherical vector-based particle swarm optimization," *Appl. Soft Comput.*, vol. 107, Aug. 2021, Art. no. 107376.
- [66] J.-H. Wang, S.-M. Lo, J.-H. Sun, Q.-S. Wang, and H.-L. Mu, "Qualitative simulation of the panic spread in large-scale evacuation," *Simulation*, vol. 88, no. 12, pp. 1465–1474, Dec. 2012.



**Tianrui Wu** received the B.S. and M.S. degrees from Shanghai Maritime University, Shanghai, China, in 2021 and 2023, respectively. His current research interests include urban emergency management, crowd evacuation, and evolutionary computation.



**Jun Yu** received the bachelor's degree from Northeastern University, China, in 2014, and the master's and Ph.D. degrees from Kyushu University, Japan, in 2017 and 2019, respectively. He is currently an Assistant Professor with Niigata University, Japan. His research interests include evolutionary computation, artificial neural networks, and machine learning.



**Qingchao Jiang** (Senior Member, IEEE) received the B.E. and Ph.D. degrees from the Department of Automation, East China University of Science and Technology, Shanghai, China, in 2010 and 2015, respectively. He is currently a Professor with the East China University of Science and Technology. From March 2015 to September 2015, he was a Post-Doctoral Fellow with the Department of Chemical and Materials Engineering, University of Alberta, Canada. From September 2015 to September 2016, he was a Humboldt Research Fel-

low with the Institute for Automatic Control and Complex Systems (AKS), University of Duisburg-Essen, Germany. His research interests include data mining and analysis, data-driven soft sensing, multivariate statistical process monitoring, and deep learning-based process modeling.

He was a recipient of the 2021 World Artificial Intelligence Conference Youth Outstanding Paper Nomination Award. He is the Early Career Advisory Board Member of the *Control Engineering Practice* (IFAC) and an Associate Editor of IEEE ACCESS.



**Qinjin Fan** received the Ph.D. degree in control science and engineering from the East China University of Science and Technology, Shanghai, China, in 2015.

He is currently an Associate Professor with Shanghai Maritime University. His current research interests include evolutionary computation, hyper-heuristic algorithm, multi-objective optimization, and their real-world applications.